Food and Chemical Toxicology 166 (2022) 113254

Contents lists available at ScienceDirect

Food and Chemical Toxicology

journal homepage: www.elsevier.com/locate/foodchemtox

Physiologically relevant curcuminoids inhibit angiogenesis *via* VEGFR2 in human aortic endothelial cells

Juan Antonio Giménez-Bastida [a,*], María Ángeles Ávila-Gálvez [a,1], Miguel Carmena-Bargueño [b], Horacio Pérez-Sánchez [b], Juan Carlos Espín [a], Antonio González-Sarrías [a]

[a] *Laboratory of Food and Health, Research Group on Quality, Safety and Bioactivity of Plant Foods, Dept. Food Science and Technology, CEBAS-CSIC, P.O. Box 164, 30100. Campus de Espinardo, Murcia, Spain*

[b] *Structural Bioinformatics and High Performance Computing Research Group (BIO-HPC), HiTech Innovation Hub, UCAM Universidad Católica de Murcia, Campus de los Jerónimos, s/n, 30107, Guadalupe, Spain*

ARTICLE INFO

Handling Editor: Dr. Jose Luis Domingo

Keywords:
Polyphenols
Migration
Cell metabolism
VEGF
Tubulogenesis

ABSTRACT

Angiogenesis is a complex process encompassing endothelial cell proliferation, migration, and tube formation. While numerous studies describe that curcumin exerts antitumor properties (e.g., targeting angiogenesis), information regarding other dietary curcuminoids such as demethoxycurcumin (DMC) and bisdemethoxycurcumin (BisDMC) is scant. In this study, we evaluated the antiangiogenic activities of these three curcuminoids at physiological concentrations (0.1–5 μM) on endothelial cell migration and tubulogenesis and the underlying associated mechanisms on human aortic endothelial cells (HAECs). Results showed that the individual compounds and a representative mixture inhibited the tubulogenic and migration capacity of endothelial cells dose-dependently, while sparing cell viability. Notably, DMC and BisDMC at 0.1 and 1 μM showed higher capacity than curcumin inhibiting tubulogenesis. These compounds also reduced phosphorylation of the VEGFR2 and the downstream ERK and Akt pathways in $VEGF_{165}$-stimulated cells. *In silico* analysis showed that curcuminoids could bind the VEGFR2 antagonizing the VEGF-mediated angiogenesis. These findings suggest that physiologically concentrations of curcuminoids might counteract pro-angiogenic stimuli relevant to tumorigenic processes.

1. Introduction

Angiogenesis refers to the formation and growth of new blood vessels from preexisting ones. This process is critically involved in physiological processes such as ovulation, embryogenesis, fetal development, and cutaneous wound healing but also contributes to developing certain pathological conditions, including tumor progression and metastasis (Carmeliet and Jain, 2011; Chung et al., 2010; Rajabi and Mousa, 2017). Angiogenesis includes endothelial cell proliferation, migration, and tube formation, providing nutrients and oxygen to cancerous cells (Potente et al., 2011; Rajabi and Mousa, 2017). Inhibition of angiogenesis is a common strategy for treating cancer progression and other diseases associated with angiogenesis (Simon et al., 2017). The use of natural compounds such as phytochemicals for angiogenesis prevention is a cost-effective method with reduced adverse side effects compared to drugs. Many (poly)phenolics compounds widely distributed in plant-derived foods such as curcumin, resveratrol, quercetin, or epigallocatechin gallate, among others, have received significant scientific attention for their potential prevention and treatment of carcinogenesis in preclinical studies, although their potential is still poorly translated to clinical trials (Ávila-Gálvez et al., 2020; Núñez-Sánchez et al., 2015). Growth inhibition, cell-cycle arrest, and apoptosis induction are multi-target activities exerted by dietary (poly)phenols on carcinogenic cell and animal models. However, most of them have not yet been tested for their antiangiogenic effects that may be partly involved in their potential prevention and(or) treatment of carcinogenesis (Abbaszadeh et al., 2019; Pan et al., 2015). Therefore, identifying and validating these antiangiogenic activities and molecular mechanisms of known dietary (poly)phenolics action is of immense interest in developing potential therapeutic targets against malignant tumors.

Turmeric (*Curcuma longa*) is a spice that contains three primary compounds known as curcuminoids, including curcumin (Curc) as the major constituent and demethoxycurcumin (DMC) and

* Corresponding author.
E-mail address: jgbastida@cebas.csic.es (J.A. Giménez-Bastida).
[1] Current address: Molecular Nutrition and Health Laboratory. CEDOC (Centro de Estudos de Doenças Crónicas), NOVA Medical School/Faculdade de Ciências Médicas, Universidade Nova de Lisboa, Edificio CEDOC II, Rua Câmara Pestana 6, 1150-082, Lisboa.

https://doi.org/10.1016/j.fct.2022.113254
Received 15 April 2022; Received in revised form 2 June 2022; Accepted 20 June 2022
Available online 23 June 2022

Abbreviations

BD	blind docking
BisDMC	bisdemethoxycurcumin
Curc	curcumin
DMC	demethoxycurcumin
DMSO	dimethyl sulfoxide;
ECBM	endothelial cell basal medium
EIC	Extracted ion chromatograms
GS	growth supplement
HAECs	human aortic endothelial cells
HBSS	Hank's balanced salt solution
HUVECs	human umbilical vein endothelial cells
ICAM-1	intracellular adhesion molecule-1
LJ	Lennard-Jones term
MeOH	methanol; Mix, mixture
MMP-9	metalloproteinase-9
MTT	3-(4,5-dimethyl-2-thiazolyl)-2,5-diphenyl-2H-tetrazolium bromide;
PBS	phosphate buffered saline;
PDB	protein data Bank
UPLC-QTOF-MS	UPLC- quadrupole-time-of-flight mass spectrometer
VEGF	vascular endothelial growth factor
VEGFR	vascular endothelial growth factor receptor

bisdemethoxycurcumin (BisDMC) as minor ones (Sharifi-Rad et al., 2020). Among them, curcumin is in the spotlight due to its antitumor properties by modulating several signaling pathways, and the molecular bases imputed to the anti-inflammatory, antiproliferative, pro-apoptotic, anti-angiogenesis, and anti-metastasis effects (Joshi et al., 2021; Slika and Patra, 2020). However, Curc, unlike other curcuminoids such as DMC, is poorly absorbed, resulting in low bioavailability (around 1% in plasma) due to its low water solubility and high chemical instability, as well as its rapid metabolism and clearance from the body, thus limiting its efficacy (Nelson et al., 2017). In this regard, a recent clinical trial conducted in newly-diagnosed breast cancer patients that consumed a mixture of phenolic extracts containing 190 mg of turmeric extract (around 65% of Curc, 25% of DMC, and 10% BisDMC) reported only 2-fold values of Curc (~5.3 nmol/L) in plasma compared to other curcuminoids (~2.4–3.9 nmol/L). Paradoxically, higher free Curc concentrations than other curcuminoids (over 10-fold) were found in the patients' malignant and normal mammary tissues (Ávila-Gálvez et al., 2021). These data suggest that in addition to Curc, other minor curcuminoids detected *in vivo* after their consumption could also display beneficial activities in the systemic environment. Nevertheless, while Curc has been reported to inhibit critical steps in tumor angiogenesis, including *in vivo* tumor growth as well as *in vitro* endothelial cell migration and proliferation *via* downregulation of vascular endothelial growth factor receptor (VEGFR), metalloproteinases, and(or) phosphodiesterases expression (Abusnina et al., 2015; Hosseini et al., 2019; Wang and Chen, 2019; Yoysungnoen et al., 2006), the antiangiogenic effects of other curcuminoids (DMC and BisDMC) remain scarcely explored (Ramezani et al., 2018; Wang and Chen, 2019).

Implantation of a pellet containing Curc, DMC, and BisDMC has been reported to inhibit the bFGF-induced corneal neovascularization in mice (Arbiser et al., 1998). Further evidence comes from *in vitro* studies that described the antiangiogenic effect of DMC and BisDMC via inhibition of proliferation and migration of endothelial cells and down-regulation of VEGF, adhesion molecules ICAM-1 (intracellular adhesion molecule-1) and MMP-9 (metalloproteinase-9) against human umbilical vein endothelial cells (HUVECs) (Huang et al., 2015; Kim et al., 2002).

Although the cancer-associated antiangiogenic effect of Curc has been previously reported in human endothelial cells, mainly in HUVEC cells (Wang and Chen, 2019), the antiangiogenic effects and the associated mechanisms in human aortic endothelial cells (HAECs) have not been described so far. HAECs are cells directly isolated from adult human aorta, retaining the morphological and functional characteristics of their tissue of origin. This makes them an excellent model to investigate cardiovascular function and disease as they closely resemble the characteristics of the tissue of origin (Endo et al., 2003; Seo et al., 2016). Besides, the antiangiogenic effects of a representative mixture containing other circulating curcuminoids to mimic the *in vivo* situation have yet to be explored. Finally, crucial angiogenesis processes such as ring-like structures formation have not yet been evaluated.

Hence, the present study aims to determine the antiangiogenic effects of the main dietary curcuminoids (Curc, DMC, and BisDMC) at physiological concentrations, evaluating their activity on migration and tubulogenesis, and underlying mechanisms targeting the key actors in angiogenesis (VEGFR, ERK, and Akt activation) in HAECs. In addition, the metabolism of each curcuminoid by HAECs is also explored.

2. Material and methods

2.1. Materials

Curcumin (Curc), demethoxycurcumin (DMC), bisdemethoxycurcumin (BisDMC) (Fig. 1), bovine serum albumin, 3-(4,5-dimethyl-2-thiazolyl)-2,5-diphenyl-2H-tetrazolium bromide (MTT) and Hanks' balanced salt solution (HBSS) were obtained from Sigma Aldrich (St. Louis, MO, USA). Endothelial cell basal medium (ECBM) and growth supplements (GS) were provided by Tebu-Bio (Barcelona, Spain). $VEGF_{165}$ was provided by R&D Systems (Minneapolis, MN, USA). Dimethyl sulfoxide (DMSO) and methanol (MeOH) were purchased from Panreac (Barcelona, Spain). Ultrapure Millipore water was used to prepare all solutions.

2.2. Cell line and culture conditions

Human aortic endothelial cells (HAECs) were purchased from the European Collection of Cell Cultures (Salisbury, UK). HAECs were cultured in endothelial cell growth medium (ECBM enriched with GS) and seeded from 5000 to 10,000 cells/cm^2 in 25-cm^2 flasks. Cells were maintained at 37 °C, 95% relative humidity, and 5% CO_2, following the manufacturer's instructions.

2.3. Dosage information

The curcuminoids tested were diluted in DMSO to obtain a 2 mM stock solution and sterilized filter (0.2 μm) prior to cell treatment. HAECs seeded at 5000 cells cm^{-1} and incubated at 37 °C were treated with DMSO (0.5% v/v) as control or Curc, DMC, BisDMC and a representative mixture (Mix) of them (87.3, 10.5 and 2.2%, respectively) at concentrations up to 10 μM for 24–27 h.

2.4. HAECs tubulogenesis

Following the procedures described elsewhere (Arnaoutova and Kleinman, 2010; Huuskes et al., 2019), we studied the effect of the compounds investigated on the tubulogenic capacity of the endothelial cells. Briefly, 96-well plates coated with cold reduced growth factor matrigel (50 μL) were incubated at 37 °C for 30 min to allow the matrigel solidification. HAECs at 80% of confluence were incubated in ECBM at 37 °C for 3 h and then trypsinized to obtain a cell solution at 2

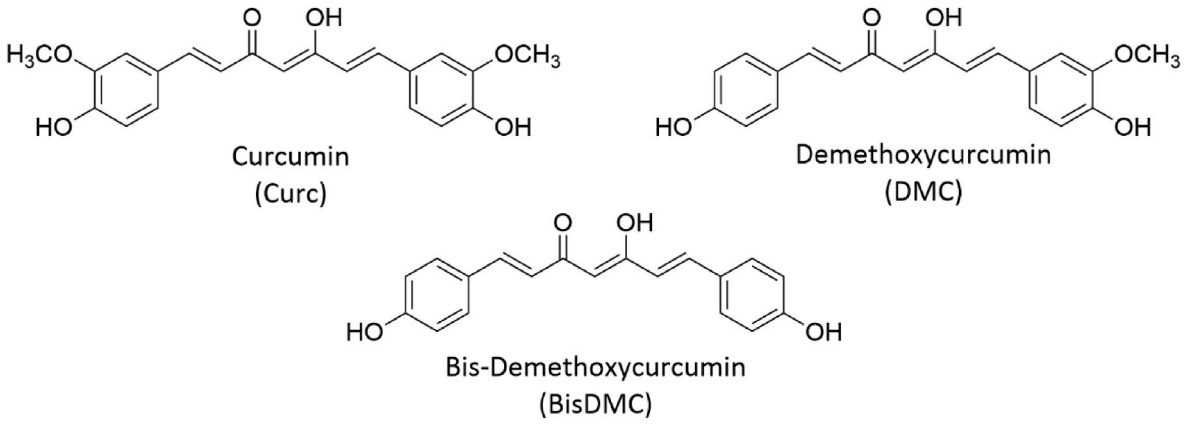

Fig. 1. Chemical structures of curcuminoids (curcumin, Curc; demethoxycurcumin, DMC; BisDMC, bisdemethoxycurcumin).

$\times 10^5$ cells/mL (concentration optimized in preliminary experiments described in supplementary material and Fig. S1) in ECBM (cell viability above 90%). Next, 50 μL cell suspension (10,000 cells) was added to each well (with solidified Matrigel) in the presence of DMSO (0.5% v/v) as control, Curc, DMC, BisDMC, and a Mix (at 5 μM) and incubated at 37 °C. After 4 h, the cells were photographed and then stimulated with GS (0.65% v/v). Additional pictures, taken at 9, 21, and 27 h using a Zeiss Fluorescence Microscope, were used to determine the effect of the compounds on tubulogenesis. One picture of each treatment (in duplicate) taken at 5x magnification was analyzed and quantified using the plug-in Angiogenesis Analyzer for Image J (Carpentier et al., 2020; DeCicco-Skinner et al., 2014) to determine the formation of endothelial rings-like structures formation. Based on the results obtained, we tested the dose-dependent effect (5, 1, and 0.1 μM) of Curc, DMC, BisDMC, and the Mix in cells treated for 21 h. The assays were repeated at least three times (n = 3).

2.5. HAECs migration

We next investigated the effect of the compounds on the capacity of the endothelial cells to migrate, as previously described (Giménez-Bastida et al., 2016; 2012). HAECs were seeded at 10,000 cells/cm^2 in 48-well plates and grown-up to confluence (≥90%). Next, the cell surface was scratched with a sterile pipet tip (200 μL), and the horizontal gap created was checked under the microscope. The medium containing displaced and dead cells was removed, and the well containing attached cells was washed with HBSS before adding fresh ECBM (GS-deprived) containing the different treatments at 5–0.1 μM or DMSO (0.5% v/v) as control. The cells were incubated with the different treatments for 4 h, followed by the addition of GS (1.5% v/v), and further incubated for 20 h (Fig. S2). From 2 to 3 pictures of each treatment were taken at 5x magnification and analyzed using the ImageJ software. The quantification of the scratched area at the different time points (4 and 24 h after the treatment with the curcuminoids or their mix) followed a method described in previous studies (Giménez-Bastida et al., 2016). The assay was repeated at least three times (n = 3).

2.6. Western blot

Confluent endothelial cells were incubated in ECBM for 3 h and treated with DMSO (0.5% v/v) as control or Curc, DMC, BisDMC, and a Mix at 5 μM for 4 h. The cells were then stimulated with 100 ng/mL $VEGF_{165}$ (diluted in 0.1% BSA in PBS, w/v) for 5 min. Cell protein extracts obtained in cold RIPA buffer supplemented with a cocktail of protease and phosphatase inhibitors (Roche, Mannheim, Germany) were kept at −80 °C until protein quantification using the DC colorimetric kit (Bio-Rad, Barcelona, Spain) and analysis by Western blot. An equal amount of protein obtained from each treatment was resolved using 8% SDS-PAGE gels and transferred to nitrocellulose membranes which were incubated with primary (1:500–1:2500 dilution) and anti-rabbit and anti-mouse secondary antibodies (1:5000 dilution) (Cell Signalling, MA, USA). The primary antibodies used were phospho (p)-VEGFR2 (Tyr1175, 19A10; #2478), total (t)-VEGFR2 (55B11; #2479), p-ERK (Thr202/Tyr204, 20G11; #4377), t-ERK (137F5; #4695), p-Akt (Ser473, 193H12; #4058) and t-Akt (C67E7; #4691). GAPDH (D4C6R; #97166) at a 1:2500 dilution was used to corroborate equal loading control. Image J was used for densitometric analysis of the protein bands, and the ratio phosphorylated/total protein (normalized to GAPDH) was used to compare the effect of the different compounds on the VEGFR2 pathway activation. The assay was repeated between 3 and 5 times (n = 3–5).

2.7. In silico analysis/Blind docking calculations

We applied the Blind Docking (BD) consensus to study the interactions of selected ligands against protein VEGFR2. The BD method determines the most likely binding hotspots for a given ligand across the selected protein surface (Tapia-Abellán et al., 2019). Regarding input file preparation, we used the crystallized structure of VEGFR2 described on the Protein Data Bank (PDB) and coded as 6GQO (https://www.rcsb.org/structure/6GQO). The processing of the PDB file using the tools of Maestro was carried out as follows: Protein Preparation Wizard allowed refining of the structure, thus avoiding clashes between atoms, and System Builder provided the information needed to obtain the charges using the OPLS3e force field (Roos et al., 2019). The format of the structure obtained was mol2.

The ligand structures (Curc, DMC, and BisDMC) in 3D sdf format were obtained from PubChem (https://pubchem.ncbi.nlm.nih.gov/). The data analysis using the tool LigPrep of Maestro provided information about each atom using the force field OPLS3e (final structures saved in mol2 format). Further processing of the molecules using the Gasteiger model with AutoDockTools converted the structures to pdbqt format. Finally, BD calculation of the files formatted as pdbqt and mol2 were performed using AutoDock Vina (Trott and Olson, 2010) and Lead Finder (Stroganov et al., 2008), respectively, using a grid box size of 30 Å^3 as default parameter. The results provided information about the distribution of binding energies and their structural clusters of poses.

The metascreener software (https://github.com/bio-hpc/metascreener) allowed to analyze the individual BDs and obtain a final BD consensus regarding superposition and the scores of both algorithms. The scoring function (of both algorithms) considered Lennard-Jones term (LJ), hydrogen bonds (H-bonds), electrostatic interactions, hydrophobic stabilization, entropic penalty due to the number of rotatable bonds, and the internal energy of each ligand. Finally, we used the Plip software (https://plip-tool.biotec.tu-dresden.de/plip-web/plip/index) to calculate the interactions between the compounds and protein

residues.

2.8. Analysis of curcuminoids metabolism in HAECs by UPLC-QTOF-MS

The capacity of the endothelial cells to metabolize the curcuminoids was studied in cell culture supernatants collected at the initial (0 h) and final points of the migration (24 h) and tubulogenesis assays (27 h). Briefly, equal volumes of culture medium (200 μL) and acetonitrile: formic acid (98:2, v/v) were mixed, vortexed, and centrifuged (14,000×*g* for 10 min). The supernatant was transferred to a new tube, dried in a Speedvac concentrator (Savant SPD 121P), and the residue reconstituted in 100 μL MeOH. A volume of 5 μL of the filtered samples (through 0.22 μm syringe filters) was used for the analysis. The identification and quantification of curcuminoids were carried out using an Agilent 1290 Infinity UPLC-ESI system coupled to a 6550 Accurate-Mass quadrupole-time-of-flight (QTOF) mass spectrometer (Agilent Technologies, Waldbronn, Germany). The conditions and parameters used are described in recent studies (Ávila-Gálvez et al., 2021). The identification and quantification of Curc, DMC, and BisDMC were acquired by using authentical standards and derived metabolites according to their accurate mass, molecular formula, and isotopic pattern. All calibration curves were obtained for each authentical standard tested, obtaining good linearity ($r^2 > 0.999$).

2.9. Statistical analysis

The software used for graphics and figures were ChemDraw Professional v. 16.0.1.4 (PerkinElmer Informatics Inc., Cambridge, MA, USA) and Sigma Plot 14.5 (Systat Software, San Jose, CA, USA), respectively. Data are shown as mean ± standard deviation (S.D.). The software used for statistical analysis was Prism 5.0 (GraphPad, La Jolla, CA, USA). Data following normal distribution (Shapiro-Wilk test) were analyzed by one-way ANOVA followed by post-hoc Dunnet analysis. Significant differences were considered at $p < 0.05$.

3. Results

3.1. Evaluation of cytotoxic activity of curcuminoids in HAECs

As shown in Fig. S3, the MTT assay revealed that concentrations below 5 μM (0.5% DMSO, v/v) exerted no cytotoxic effects. Based on these results, the experiments were carried out using concentrations ranging from 0.1 to 5 μM to discard any effect associated with cytotoxicity.

3.2. Curcuminoids inhibit tubulogenesis in stimulated HAECs

We analyzed the inhibitory effect of Curc, DMC, and BisDMC individually and a mix (Mix) of these compounds (at 5 μM) on the tubulogenic capacity (measured as the number of rings formed) of HAECs at different time points (Fig. 2). In the absence of pro-angiogenic factors, there were no differences between the cells pre-treated with the curcuminoids (individually or the Mix) for 4 h and the untreated cells (Fig. 2B). However, after the 4 h pretreatment, the GS-stimulated cells increased the formation of the ring-like structures over the incubation time. Besides, Curc, DMC, BisDMC, and Mix at 5 μM exerted a significant inhibition of the formation of the rings at the different time points (Fig. 2A and B). Based on these results, we also studied whether lower concentrations (1 and 0.1 μM) effectively inhibited tubulogenesis at 21 h of (maximum difference compared with the stimulated cells; Fig. 2B). However, Curc did not inhibit tubulogenesis at concentrations below 5 μM (Fig. 3, Fig. S4). Notably, DMC and BisDMC exerted a similar significant inhibitory effect at the concentrations investigated (5–0.1 μM; $p < 0.05$), whereas a significant reduction in the Mix-treated cells was observed at 5 and 1 μM ($p < 0.05$) (Fig. 3D, Fig. S4).

3.3. Curcuminoids inhibit endothelial cell migration

We next determined whether the compounds investigated showed the capacity to inhibit the endothelial cell migration. As expected, the treatment of the endothelial cells with GS induced endothelial cells migration more clearly than the unstimulated cells (Fig. 4A and B). Results showed significant migration inhibition in the presence of the individual compounds or the Mix at 5 μM (Fig. 4A and B). A reduction in cell migration appeared visually evident in the presence of DMC and BisDMC at 1 and 0.1 μM (Fig. S5), although the statistical analysis of the data showed no significant differences (Fig. 4B). At these lower concentrations, the inhibitory effect of Curc and the Mix was much less clear (Fig. 4; Fig. S5).

3.4. VEGFR2 pathway inhibition by curcuminoids

Additional experiments related to studying the molecular mechanisms by which the curcuminoids exerted their effects focused on the VEGFR2 pathway (Fig. 5). Western blot analysis of the $VEGF_{165}$-treated HAECs' protein showed activation of the VEGFR2 via Y1175 phosphorylation. The activation of the VEGFR2 paralleled higher phosphorylation levels of ERK (Thr202/Tyr204) and Akt (Ser473). The pretreatment of the cells with the individual curcuminoids or the Mix (5 μM, 4 h) down-regulated the $VEGF_{165}$-induced VEGFR2 phosphorylation at the Y1175 site, and in turn the ERK and Akt's phosphorylation levels (Fig. 5A and B).

3.5. In silico/molecular modeling of protein-ligand interactions via Blind Docking

Results revealed that Curc, DMC, and BisDMC showed similar binding poses located at the same sites of the VEGFR2. Identifying the key residues of VEGFR2 involved in Curc, DMC and BisDMC using the BD analysis showed multiple protein-ligand interaction hotspots with different docking scores (Fig. 6A). The binding hotspot with the highest docking score (obtained from the top-ranked values of each ligand obtained using both algorithms) showed values between −9 and −11 kcal/mol, suggesting that it is the most likely one involved in the ligand-receptor interaction. Fig. 6B displays the predicted key amino acids for binding to BisDMC (the molecule that shows the highest number of interactions). Table S1 summarizes the critical residues involved in the interaction of curcuminoids to VEGFR2 and shows joint interactions between the three compounds and several residues of the protein (see Fig. 6).

3.6. Curcuminoids metabolism by HAECs

Chromatographic analysis by UPLC-QTOF-MS of Curc, DMC, and BisDMC individually and the Mix (5 μM) revealed that all compounds were stable in the media before and after the incubation with the HAECs (data not shown). Fig. 7 shows representative extracted ion chromatograms (EICs) of Cur, DMC, and BisDMC at the initial (0 h) and final (27 h) time points of incubation carried out in the tubulogenesis assay. The chromatograms of the DMC and BisDMC samples showed no differences between the time 0 and 27 h samples. Analysis of Curc and Mix samples after 27 h incubation gave one additional peak compared to time 0. This ion at m/z^- 447.0755 (mass error = −0.32 ppm) ($C_{21}H_{20}O_9S$) was tentatively identified as Curc sulfate (Fig. 7A). The conversion degree of Curc to Curc sulfate was between 1 and 4% yield in the Curc and Mix samples obtained from the migration or tubulogenesis assays.

4. Discussion

Turmeric is a spice obtained from *Curcuma longa* traditionally used to prevent and treat chronic diseases such as breast cancer (Gupta et al., 2013; Kalluru et al., 2022). Interest in its health benefits has primarily

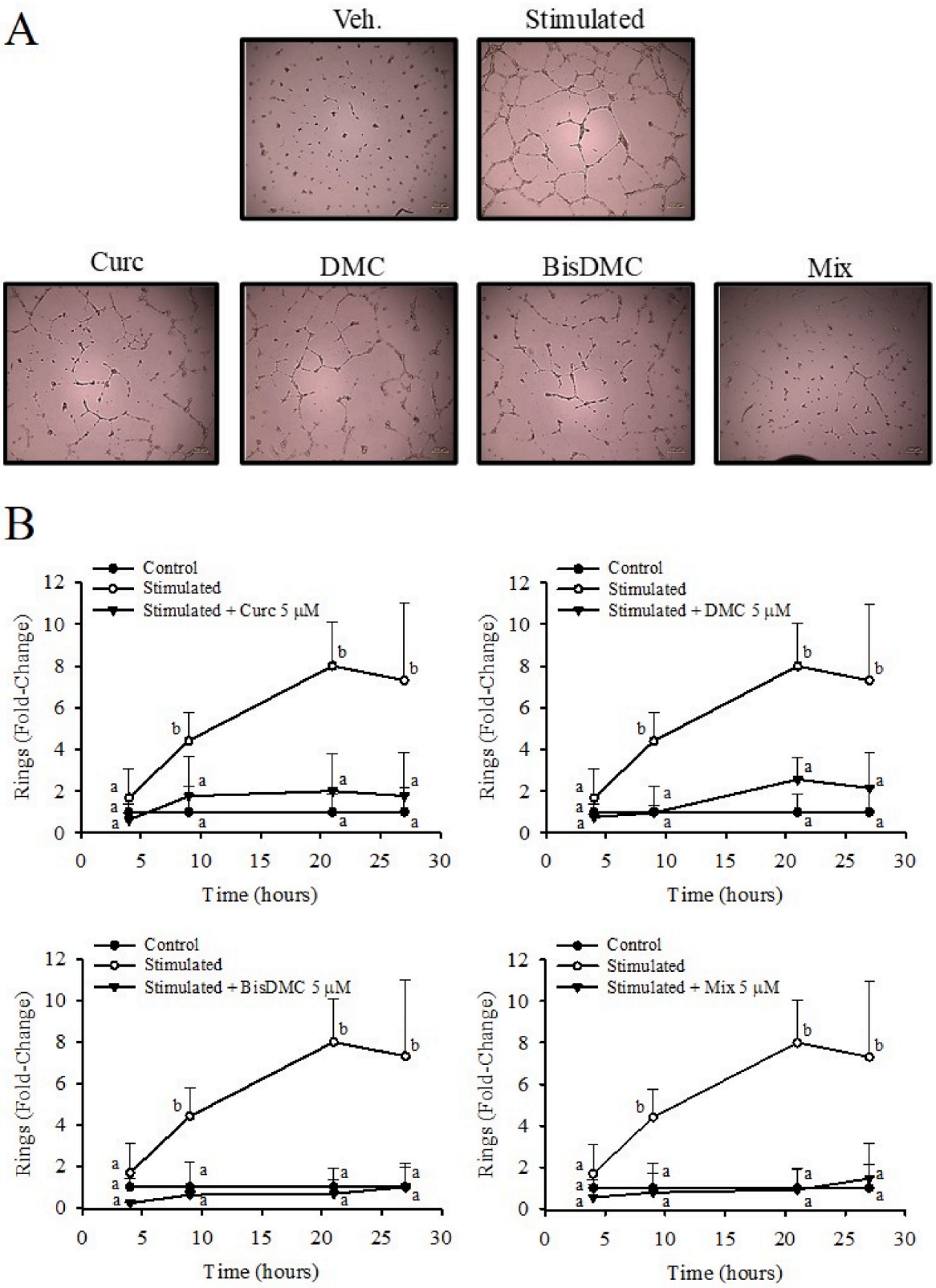

Fig. 2. Time course effect of Curc, DMC, BisDMC, and the Mix on HAECs tubulogenesis. The cells pre-treated with the compounds for 4 h followed by the stimulation with GS (1.5% v/v) were photographed at different time points. A) Representative images of the ring-like structures formed by the cells treated with DMSO (vehicle, Veh.) in the absence of GS (control), or DMSO, Curc, DMC, BisDMC, and the Mix at 5 μM in the presence of 1.5% GS after 21 h of treatment. B) Quantification of the rings network formed at the different time points using the Angiogenesis Analyzer Plug-in for ImageJ software. The results are shown as mean ± standard deviation (SD) and calculated as fold-change relative to Veh.-treated cells (set as 1). The graphics result from three different experiments (n = 3). Each treatment was carried out in duplicate. Different letters indicate significant differences ($p < 0.05$) between the treatments at each time point.

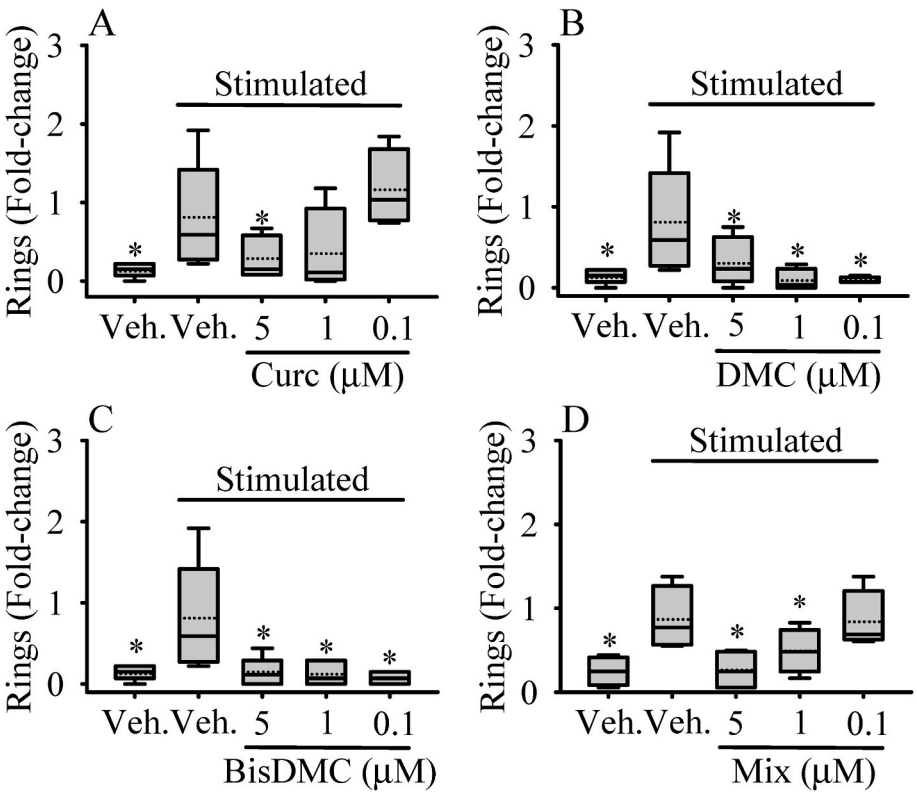

Fig. 3. Dose-dependent effect of Curc (A), DMC (B), BisDMC (C) and the Mix (D) on HAECs tubulogenesis. The cells were pre-treated with the compounds (from 0.1 to 5 μM for 4 h), then stimulated with 1.5% GS (v/v), and photographed after 21 h of treatment. Rings network formation was quantified using the Angiogenesis Analyzer Plug-in for ImageJ software, and the results were expressed as fold-change relative to stimulated cells (set as 1). The results are shown as box plots that include the median and the mean (solid and dashed horizontal lines, respectively). The box plots result from at least four different experiments (n = 4). Each treatment was carried out in duplicate. Significant differences compared to the stimulated cells are shown as: *$p < 0.05$.

focused on the naturally occurring curcuminoids. Identifying and quantifying the molecules found in human tissues (Ávila-Gálvez et al., 2021) set the basis to investigate their cellular and molecular mechanisms against cancer. Thus, a representative mixture of the breast-tissue occurring curcuminoids at 10 μM inhibited cell proliferation and induced senescence, apoptosis, and cell cycle arrest in breast cancer cell lines (Ávila-Gálvez et al., 2021). In addition to tumor cells, targeting normal cells involved in angiogenesis is considered a promising strategy against cancer (Ferrara and Kerbel, 2005). Tubulogenesis and endothelial cell migration are effective *in vitro* assays to investigate the capacity of a molecule(s) to inhibit or stimulate angiogenesis. In this study, we set out to compare the antiangiogenic activity of individual curcuminoids and a Mix at physiologically relevant concentrations in HAECs.

Under our assay conditions, a representative Mix of curcuminoids (containing 87.3% of Curc) and individual Curc exerted a similar dose-dependent inhibition (significant effect only at 5 μM in both treatments) on endothelial tubulogenesis and migration. These results, together with the overwhelming (preclinical and clinical) evidence related to the antiangiogenic potential of Curc (Gururaj et al., 2002; Shakeri et al., 2019; Yadav and Aggarwal, 2011; Yoysungnoen-Chintana et al., 2014) suggest that this molecule is the main responsible for the observed effects in the presence of the Mix. Nevertheless, some investigations imply DMC and BisDMC as potent (or even more) than Curc (Edwards et al., 2020; Kao et al., 2021; Yoon et al., 2014). Interestingly, our results showed that DMC and BisDMC exerted a potent inhibition on the formation of ring-like structures at the lowest concentrations tested (from 0.1 to 1 μM). These low concentrations are present in the Mix (1 and 5 μM), suggesting their contribution to the effects exerted by the Mix. Our results further showed a dose-dependent reduction of HAECs migration upon treatment with DMC and BisDMC, although the effect was only significant at 5 μM. A conceivable mechanism to explain the stronger effects exerted by these molecules on tubulogenesis compared to migration might involve inhibition of the Akt pathway. For example, 10–30 μM Curc blocked the PI3K/Akt/mTOR signaling in hepatocyte growth factor (HGF)-stimulated HUVECs, what resulted in a strong tubulogenesis inhibition and a weak inhibition of endothelial migration (Jiao et al., 2016).

In agreement with our results, previous studies support the inhibitory effect of Curc on endothelial tubulogenesis and migration (Binion et al., 2008; Jiao et al., 2016; Shankar et al., 2007). However, these studies assayed concentrations between 10 and 60 μM (higher than those used in this study), which are unlikely to be detected *in vivo* after curcuminoids-rich foods intake (Asai and Miyazawa, 2000; Ávila-Gálvez et al., 2021; Kunihiro et al., 2019; Mahale et al., 2018). Besides, such high concentrations could affect HAECs viability (Fig. S3). At similar concentrations, 1 μM Curc exerted a potent inhibition (similar effect observed at 50 μM) of endothelial tubulogenesis and migration (Astinfeshan et al., 2019; Hosseini et al., 2019), whereas these effects were not significant in our study. A possible explanation for these discrepancies might be the different cell lines used. HUVECs is a widely approached cellular model (used in the studies described above) to investigate processes related to angiogenesis. However, this cell line might show significant differences compared to the adult vascular endothelium (Tan et al., 2004; Wang et al., 2021), whereas the endothelial cells used in our study come from a healthy human aorta, making it them excellent as angiogenesis *in vitro* model (Endo et al., 2003; Seo et al., 2016). These differences could also explain why concentrations above 5 μM are cytotoxic to HAECs, yet not to HUVECs (Fu et al., 2015; Sheu et al., 2013).

There is appreciably less information regarding the antiangiogenic effects of DMC and BisDMC. Our results agree with precedent studies describing their capacity to inhibit *in vivo* and *ex vivo* neovascularization (Arbiser et al., 1998; Huang et al., 2015; Kim et al., 2002), and *in vitro* endothelial migration (Huang et al., 2015; Sheu et al., 2013). However, the concentrations assayed (11–52 μM) were higher than those used in our assays. Evidence on the role of DMC and BisDMC on tubulogenesis is limited, and our study describes for the first time their antiangiogenic effects on HAECs.

Cells of the vascular system can be involved in the metabolism of phenolic compounds through the hydrolysis (Fernández-Castillejo et al.,

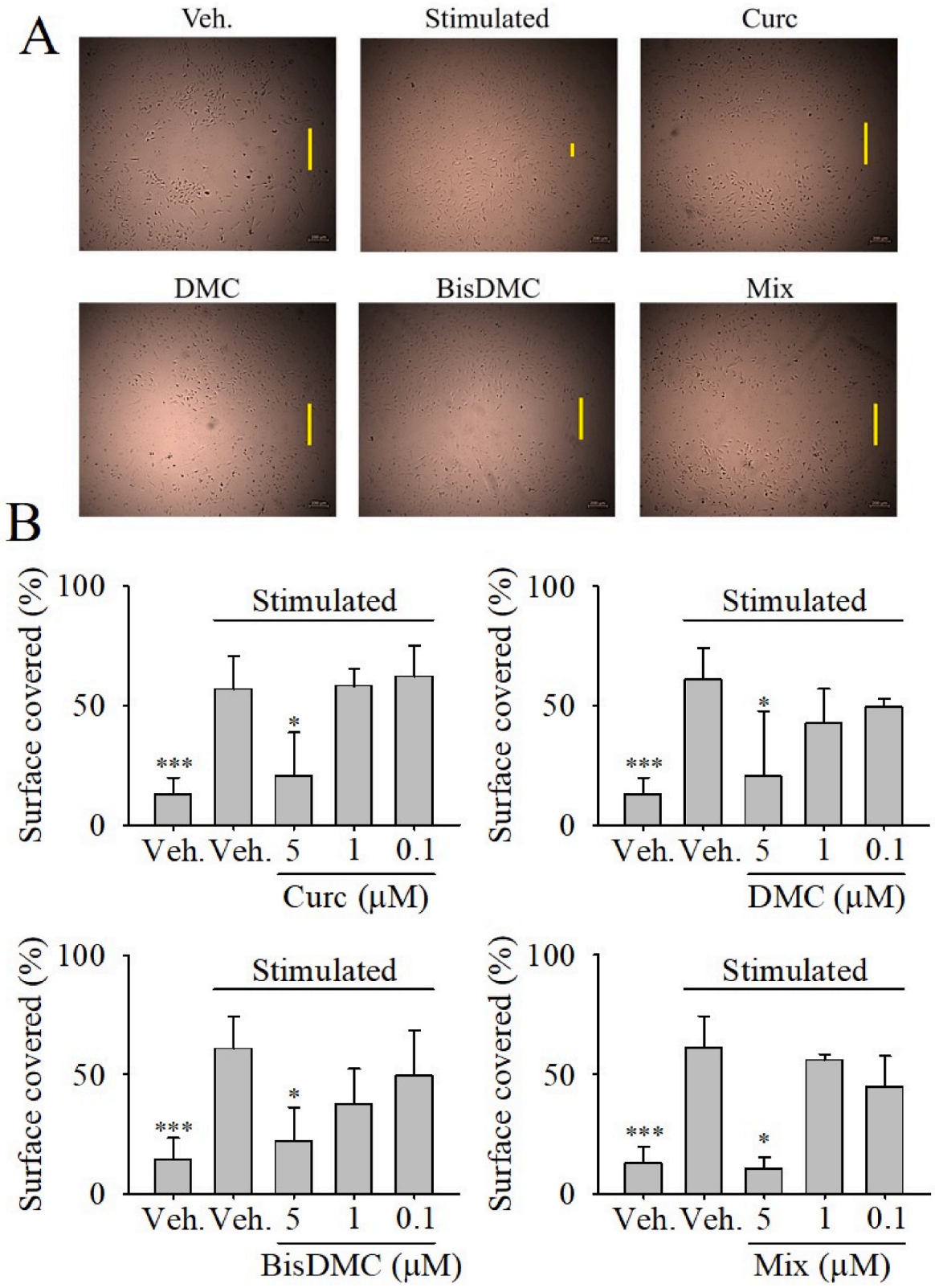

Fig. 4. Effect of Curc, DMC, BisDMC, and the Mix on HAECs migration. (A) Representative images of the effect of curcuminoids at 5 μM on the capacity of the endothelial cells to migrate after 24 h of treatment in the absence (Veh.-treated cells) or presence (rest of the treatments) of 1.5% GS (v/v). B) Quantification of the migration capacity of stimulated endothelial cells treated with (A) Curc, (B) DMC, (c) BisDMC, and (D) the Mix at concentrations from 0.1 to 5 μM for 24 h. The bar graphs show the mean ± SD of at least 3 different experiments (n = 3). Each treatment was carried out in duplicates. Significant differences compared to the stimulated cells are showed as: ***$p < 0.001$; *$p < 0.05$.

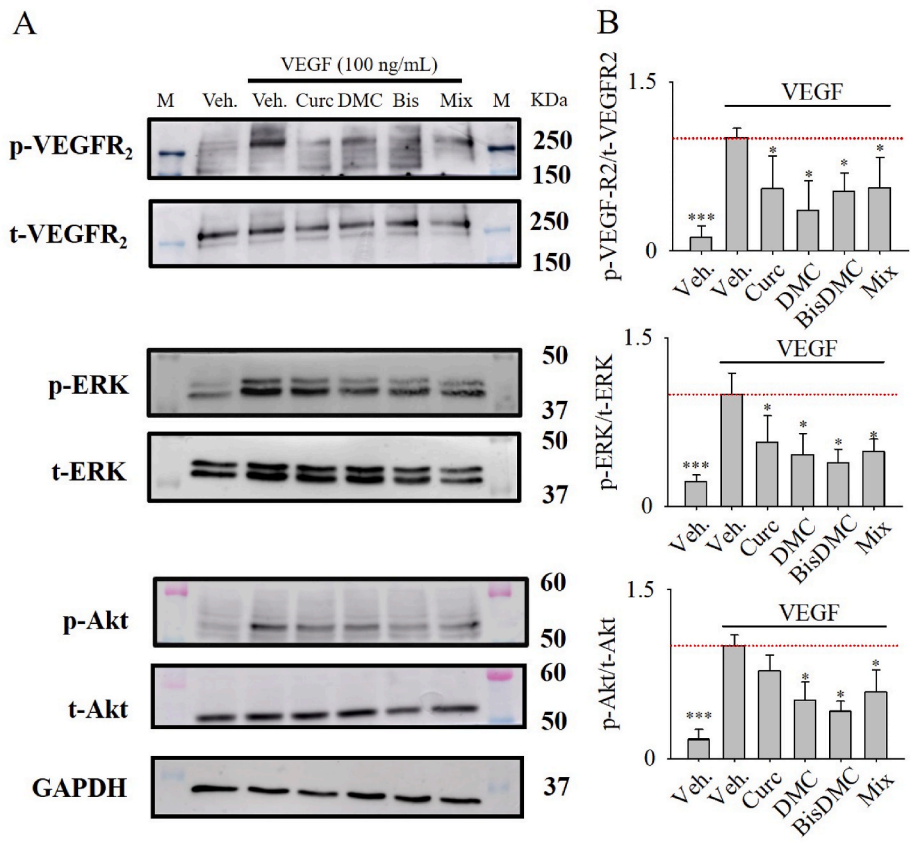

Fig. 5. Western blot analysis of phosphorylation level of VEGFR2 (p-VEGFR2/t-VEGFR2) and the downstream proteins ERK (p-ERK/t-ERK) and Akt (p-Akt/t-Akt) in HAECs. (A) Representative Western blot images of the proteins investigated. The level of phosphorylated, total protein, and GAPDH (loading control) was quantified by densitometry using ImageJ software. (B) The phosphorylated/total protein (normalized to GAPDH) ratio was used to determine the pathway's activation. The bar graphs show the mean ± SD of at least 3 different experiments (n = 3). Significant differences compared to the stimulated cells are showed as: ***p < 0.001; *p < 0.05.

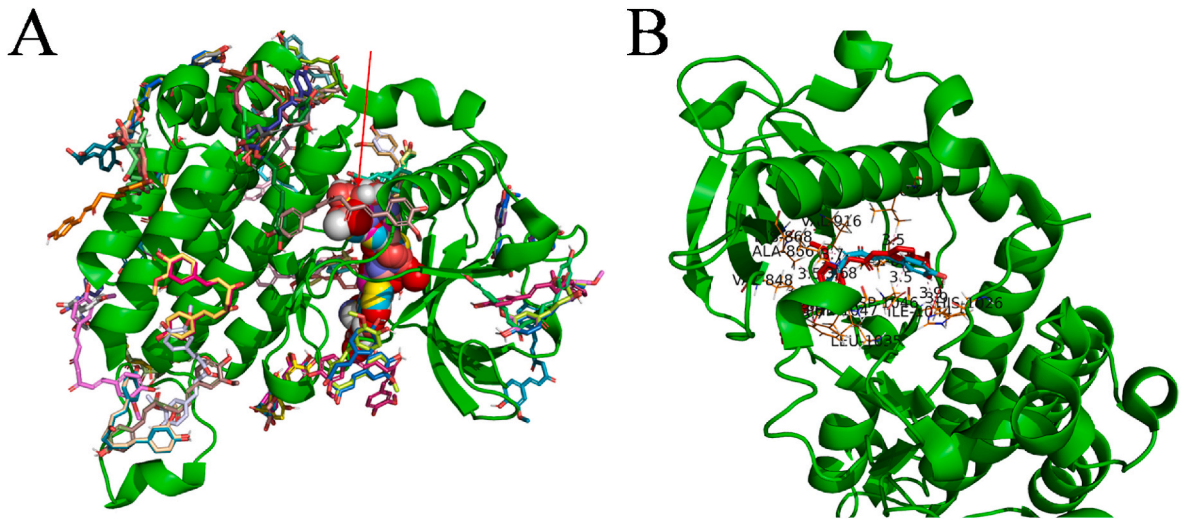

Fig. 6. (A) Blind Docking complex and (B) first metacluster as results of the BD consensus. Illustrative images were prepared using the PyMOL software. The metacluster (interaction with BisDMC calculated with the LF algorithm) is shown as a representative example. The crystal complex 6GQO is included for comparing our BD results with prior studies.

2019; Menendez et al., 2011) or biosynthesis (Giménez-Bastida et al., 2016) of phase-II metabolites. Curcuminoids metabolism analysis by UPLC-QTOF-MS showed the formation of a Curc-sulfate metabolite. However, the possible contribution of this conjugated metabolite to the *in vitro* effects seems unlikely due to the low amount generated (1–4% yield) and the low activity compared to its Curc precursor (Ireson et al., 2001).

VEGF and its receptor VEGFR2 constitute a well-characterized pathway that plays a pivotal role in angiogenesis (Abhinand et al., 2016). VEGF binds the VEGFR2 and activates downstream pathways (i.e., p38, ERK, and Akt, among others), promoting cell migration and tubulogenesis in HAECs (Endo et al., 2003). Considering that selective VEGFR2 inhibition hampers the VEGF-induced endothelial tubulogenesis and migration (Endo et al., 2003), we explored whether Cur, DMC, BisDMC, and the Mix might exert their inhibitory effects by targeting the VEGF/VEGFR2 pathway. According to previous studies (Ejaz et al., 2009; Wang et al., 2015), a possible mechanism for inhibition of angiogenesis by curcuminoids is the down-regulation of VEGFR2.

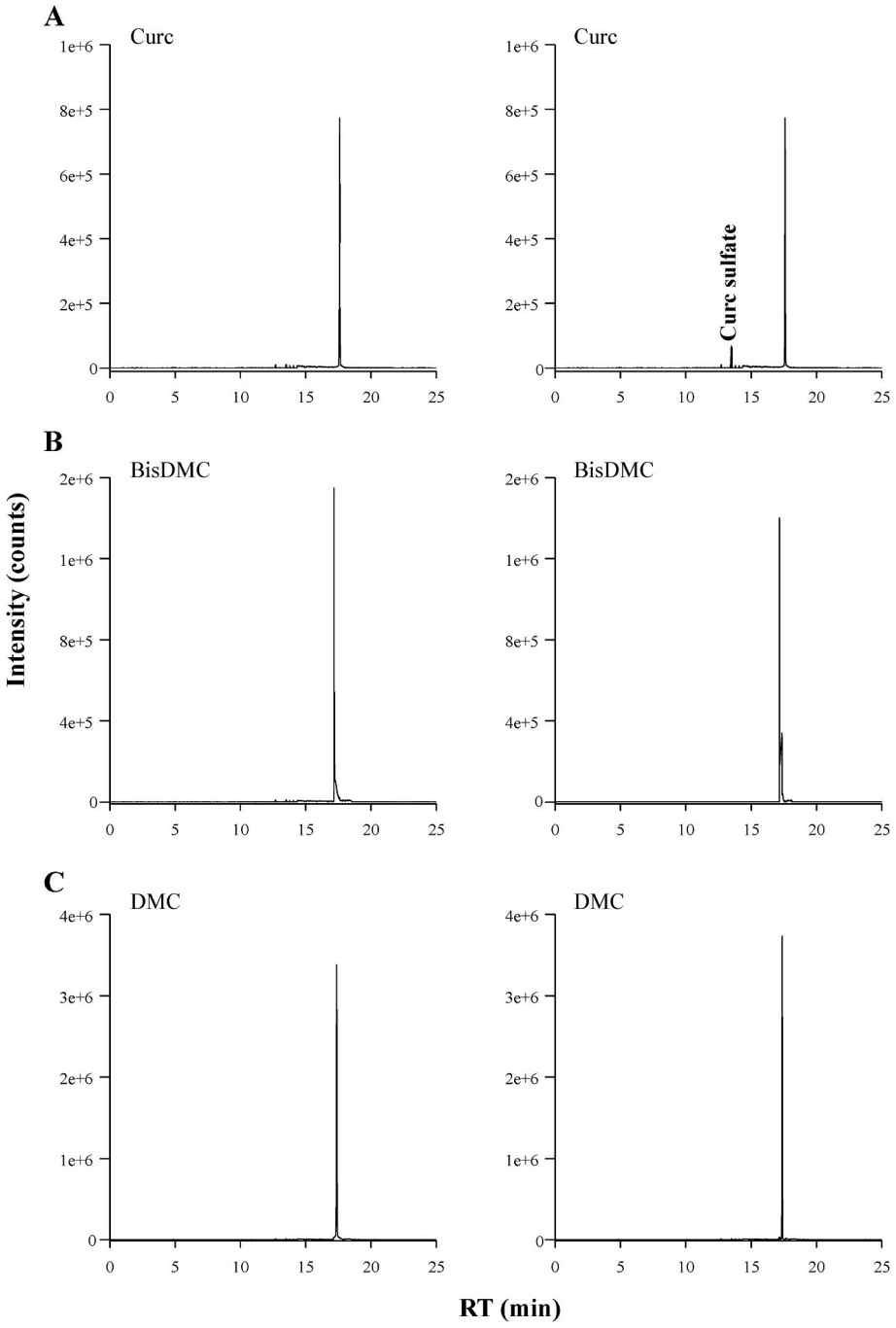

Fig. 7. UPLC-ESI-QTOF-MS extracted-ion chromatograms (EICs) of Curc, DMC, and BisDMC. EICs were obtained from HAECs tubulogenesis assay at the initial (0 h; left chromatograms) and final time point (27 h; right chromatograms). (**A**) The panel shows the EICs of Curc (RT = 17.60 min) and the m/z^- at 447.0755 obtained after 27 h and identified as Curc sulfate (RT = 13.45 min). (**B**) EICs from BisDMC (RT = 17.15 min). (**C**) EICs from DMC (RT = 17.38 min).

However, the individual compounds and their mixture lacked effect on the receptor expression. Another possible mechanism is related to inhibiting its activation via phosphorylation (Cerezo et al., 2015; Fu et al., 2015). Curc, DMC, BisDMC, and the Mix were equally potent in inhibiting phosphorylation of Y1175, an essential residue for VEGFR2 activation and modulation of the endothelial angiogenic activity (Wang et al., 2020). This inhibitory effect resulted, in turn, in the blockage of downstream pathways involved in angiogenesis modulation, such as ERK and Akt (Endo et al., 2003). These effects confirmed previous studies describing that Curc inhibits processes related to angiogenesis targeting the VEGF/VEGFR2 pathway in HUVECs (Koo et al., 2015). On the other hand, whether the curcuminoids exert their effect through the interaction with VEGFR2 was explored using *in silico* assays. Classical or focused docking methodologies are limited since they confine their exploration area to restricted or specifics sites of the protein surface. The BD approach allows exploring the whole protein surface to find additional or even allosteric interaction sites, determining an interaction probability. Our *in silico* results indicate that Curc, DMC, and BisDMC might exert their inhibitory effects binding the receptor and blocking the VEGF activity in HAECs. The two different docking algorithms used in the BD consensus approach predicted common interaction hotspots between the VEGFR2 and the curcuminoids tested. Notably, the first predicted hotspot shows similarities to the one reported for the VEGFR2 inhibitor AZD3229 (Kettle et al., 2018). Also, the residues included in

Table S1 were similar to those found in the crystal structure of the compound 6GCO (Kettle et al., 2018). To the best of our knowledge, studies focused on the effect of Curc, DMC, and BisDMC on VEGFR2 activation have not been conducted, let alone the investigation of a representative mixture of curcuminoids. Thus, additional information about the interaction between the curcuminoids and VEGFR2 is critical to understanding the molecular mechanisms related to their effects, justifying the design of future studies following relevant approaches described in prior studies (Harada et al., 2022).

5. Conclusion

While Curc has been extensively explored, other minor but bioavailable curcuminoids, such as DMC and BisDMC, and a representative mixture of them, have been reported, for the first time, to exert antiangiogenic activities at physiological concentrations (0.1–5 μM), on endothelial cell migration and tubulogenesis of HAECs. Another important finding is the identification of VEGFR2 as a molecular target of the three curcuminoids. Our study describes how the curcuminoids bind the VEGFR2 (based on an *in silico* analysis), acting as VEGF antagonists, enlarging our comprehension of the molecular mechanisms related to their antiangiogenic effects. Overall, the present data show that physiologically plausible concentrations of dietary curcuminoids might counteract pro-angiogenic stimuli relevant to tumorigenic processes, giving new perspectives for *in vivo* translational studies.

CRediT authorship contribution statement

Juan Antonio Giménez-Bastida: Conceptualization, designed the study, Methodology, Validation, Formal analysis, Data curation, Investigation, and, Software, Resources, all authors provided study material, samples, instrumentation, computing resources, or other analysis tools, Writing – original draft, Writing – review & editing, All authors analyzed the results and approved the final version of the manuscript, Visualization. **María Ángeles Ávila-Gálvez:** Formal analysis, Resources, performed all the experiments, except for those related to the in silico analysis, which were performed by, Resources: all authors provided study material, samples, instrumentation, computing resources, or other analysis tools, Writing – review & editing, All authors analyzed the results and approved the final version of the manuscript; chromatograms prepared by. **Miguel Carmena-Bargueño:** Formal analysis, Resources, Writing – review & editing, performed all the experiments, except for those related to the in silico analysis, which were performed by, Resources: all authors provided study material, samples, instrumentation, computing resources, or other analysis tools; Writing – Review & Editing: All authors analyzed the results and approved the final version of the manuscript; prepared all the graphics except the in silico figures prepared by. **Horacio Pérez-Sánchez:** Formal analysis, Resources, Writing – review & editing, performed all the experiments, except for those related to the in silico analysis, which were performed by, Resources: all authors provided study material, samples, instrumentation, computing resources, or other analysis tools; Writing – Review & Editing: All authors analyzed the results and approved the final version of the manuscript; prepared all the graphics except the in silico figures prepared by. **Juan Carlos Espín:** Formal analysis, Resources, Writing – review & editing, Conceptualization, Resources: all authors provided study material, samples, instrumentation, computing resources, or other analysis tools; Writing – Review & Editing: All authors analyzed the results and approved the final version of the manuscript. **Antonio González-Sarrías:** Conceptualization, Formal analysis, Writing – original draft, Conceptalization: contributed to performing the chromatographic analysis and maintaining the cell line; wrote the manuscript with the help of the rest of the authors.

Declaration of competing interest

The authors declare that they have no known competing financial interests or personal relationships that could have appeared to influence the work reported in this paper.

Acknowledgments

J.A.G.-B. was supported by Standard European Marie Curie Individual Fellowship from the European Commission. This project has received funding from the European Union's Horizon 2020 research and innovation programme under the Marie Sklodowska-Curie Grant Agreement No 838991, and by the project PID2019-103914RB-I00 from the Ministry of Science and Innovation (MICINN, Spain).

Appendix A. Supplementary data

Supplementary data to this article can be found online at https://doi.org/10.1016/j.fct.2022.113254.

References

Abbaszadeh, H., Keikhaei, B., Mottaghi, S., 2019. A review of molecular mechanisms involved in anticancer and antiangiogenic effects of natural polyphenolic compounds. Phytother Res. 33, 2002–2014. https://doi.org/10.1002/ptr.6403.

Abhinand, C.S., Raju, R., Soumya, S.J., Arya, P.S., Sudhakaran, P.R., 2016. VEGF-A/VEGFR2 signaling network in endothelial cells relevant to angiogenesis. J. Cell Commun. Signal 10, 347–354. https://doi.org/10.1007/s12079-016-0352-8.

Abusnina, A., Keravis, T., Zhou, Q., Justiniano, H., Lobstein, A., Lugnier, C., 2015. Tumour growth inhibition and antiangiogenic effects using curcumin correspond to combined PDE2 and PDE4 inhibition. Thromb. Haemostasis 113, 319–328. https://doi.org/10.1160/TH14-05-0454.

Arbiser, J.L., Klauber, N., Rohan, R., van Leeuwen, R., Huang, M.T., Fisher, C., Flynn, E., Byers, H.R., 1998. Curcumin is an in vivo inhibitor of angiogenesis. Mol. Med. 4, 376–383.

Arnaoutova, I., Kleinman, H.K., 2010. In vitro angiogenesis: endothelial cell tube formation on gelled basement membrane extract. Nat. Protoc. 5, 628–635. https://doi.org/10.1038/nprot.2010.6.

Asai, A., Miyazawa, T., 2000. Occurrence of orally administered curcuminoid as glucuronide and glucuronide/sulfate conjugates in rat plasma. Life Sci. 67, 2785–2793. https://doi.org/10.1016/s0024-3205(00)00868-7.

Astinfeshan, M., Rasmi, Y., Kheradmand, F., Karimipour, M., Rahbarghazi, R., Aramwit, P., Nasirzadeh, M., Daeihassani, B., Shirpoor, A., Gholinejad, Z., Saboory, E., 2019. Curcumin inhibits angiogenesis in endothelial cells using downregulation of the PI3K/Akt signaling pathway. Food Biosci. 29, 86–93. https://doi.org/10.1016/j.fbio.2019.04.005.

Ávila-Gálvez, M.Á., Giménez-Bastida, J.A., Espín, J.C., González-Sarrías, A., 2020. Dietary phenolics against breast cancer. A critical evidence-based review and future perspectives. Int. J. Mol. Sci. 21, E5718. https://doi.org/10.3390/ijms21165718.

Ávila-Gálvez, M.Á., González-Sarrías, A., Martínez-Díaz, F., Abellán, B., Martínez-Torrano, A.J., Fernández-López, A.J., Giménez-Bastida, J.A., Espín, J.C., 2021. Disposition of dietary polyphenols in breast cancer patients' tumors, and their associated anticancer activity: the particular case of curcumin. Mol. Nutr. Food Res. 65, e2100163 https://doi.org/10.1002/mnfr.202100163.

Binion, D.G., Otterson, M.F., Rafiee, P., 2008. Curcumin inhibits VEGF-mediated angiogenesis in human intestinal microvascular endothelial cells through COX-2 and MAPK inhibition. Gut 57, 1509–1517. https://doi.org/10.1136/gut.2008.152496.

Carmeliet, P., Jain, R.K., 2011. Molecular mechanisms and clinical applications of angiogenesis. Nature 473, 298–307. https://doi.org/10.1038/nature10144.

Carpentier, G., Berndt, S., Ferratge, S., Rasband, W., Cuendet, M., Uzan, G., Albanese, P., 2020. Angiogenesis analyzer for ImageJ - a comparative morphometric analysis of "endothelial tube formation assay" and "Fibrin Bead assay.". Sci. Rep. 10, 11568 https://doi.org/10.1038/s41598-020-67289-8.

Cerezo, A.B., Winterbone, M.S., Moyle, C.W.A., Needs, P.W., Kroon, P.A., 2015. Molecular structure-function relationship of dietary polyphenols for inhibiting VEGF-induced VEGFR-2 activity. Mol. Nutr. Food Res. 59, 2119–2131. https://doi.org/10.1002/mnfr.201500407.

Chung, A.S., Lee, J., Ferrara, N., 2010. Targeting the tumour vasculature: insights from physiological angiogenesis. Nat. Rev. Cancer 10, 505–514. https://doi.org/10.1038/nrc2868.

DeCicco-Skinner, K.L., Henry, G.H., Cataisson, C., Tabib, T., Gwilliam, J.C., Watson, N.J., Bullwinkle, E.M., Falkenburg, L., O'Neill, R.C., Morin, A., Wiest, J.S., 2014. Endothelial cell tube formation assay for the in vitro study of angiogenesis. J. Vis. Exp., e51312 https://doi.org/10.3791/51312.

Edwards, R.L., Luis, P.B., Nakashima, F., Kunihiro, A.G., Presley, S.-H., Funk, J.L., Schneider, C., 2020. Mechanistic differences in the inhibition of NF-κB by turmeric and its curcuminoid constituents. J. Agric. Food Chem. 68, 6154–6160. https://doi.org/10.1021/acs.jafc.0c02607.

Ejaz, A., Wu, D., Kwan, P., Meydani, M., 2009. Curcumin inhibits adipogenesis in 3T3-L1 adipocytes and angiogenesis and obesity in C57/BL mice. J. Nutr. 139, 919–925. https://doi.org/10.3945/jn.108.100966.

Endo, A., Fukuhara, S., Masuda, M., Ohmori, T., Mochizuki, N., 2003. Selective inhibition of vascular endothelial growth factor receptor-2 (VEGFR-2) identifies a central role for VEGFR-2 in human aortic endothelial cell responses to VEGF. J. Recept. Signal Transduct. Res. 23, 239–254. https://doi.org/10.1081/rrs-120025567.

Fernández-Castillejo, S., Macià, A., Motilva, M.-J., Catalán, Ú., Solà, R., 2019. Endothelial cells deconjugate resveratrol metabolites to free resveratrol: a possible role in tissue factor modulation. Mol. Nutr. Food Res. 63, e1800715 https://doi.org/10.1002/mnfr.201800715.

Ferrara, N., Kerbel, R.S., 2005. Angiogenesis as a therapeutic target. Nature 438, 967–974. https://doi.org/10.1038/nature04483.

Fu, Z., Chen, X., Guan, S., Yan, Y., Lin, H., Hua, Z.-C., 2015. Curcumin inhibits angiogenesis and improves defective hematopoiesis induced by tumor-derived VEGF in tumor model through modulating VEGF-VEGFR2 signaling pathway. Oncotarget 6, 19469–19482. https://doi.org/10.18632/oncotarget.3625.

Giménez-Bastida, J.A., González-Sarrías, A., Vallejo, F., Espín, J.C., Tomás-Barberán, F. A., 2016. Hesperetin and its sulfate and glucuronide metabolites inhibit TNF-α induced human aortic endothelial cell migration and decrease plasminogen activator inhibitor-1 (PAI-1) levels. Food Funct. 7, 118–126. https://doi.org/10.1039/c5fo00771b.

Giménez-Bastida, J.A., Larrosa, M., González-Sarrías, A., Tomás-Barberán, F., Espín, J.C., García-Conesa, M.-T., 2012. Intestinal ellagitannin metabolites ameliorate cytokine-induced inflammation and associated molecular markers in human colon fibroblasts. J. Agric. Food Chem. 60, 8866–8876. https://doi.org/10.1021/jf300290f.

Gupta, S.C., Sung, B., Kim, J.H., Prasad, S., Li, S., Aggarwal, B.B., 2013. Multitargeting by turmeric, the golden spice: from kitchen to clinic. Mol. Nutr. Food Res. 57, 1510–1528. https://doi.org/10.1002/mnfr.201100741.

Gururaj, A.E., Belakavadi, M., Venkatesh, D.A., Marmé, D., Salimath, B.P., 2002. Molecular mechanisms of antiangiogenic effect of curcumin. Biochem. Biophys. Res. Commun. 297, 934–942. https://doi.org/10.1016/s0006-291x(02)02306-9.

Harada, N., Okuyama, M., Teraoka, Y., Arahori, Y., Shinmori, Y., Horiuchi, H., Luis, P.B., Joseph, A.I., Kitakaze, T., Matsumura, S., Hira, T., Yamamoto, N., Iuni, T., Goshima, N., Schneider, C., Inui, H., Yamaji, R., 2022. Identification of G protein-coupled receptor 55 (GPR55) as a target of curcumin. NPJ Sci. Food 6, 4. https://doi.org/10.1038/s41538-021-00119-x.

Hosseini, A., Rasmi, Y., Rahbarghazi, R., Aramwit, P., Daeihassani, B., Saboory, E., 2019. Curcumin modulates the angiogenic potential of human endothelial cells via FAK/P-38 MAPK signaling pathway. Gene 688, 7–12. https://doi.org/10.1016/j.gene.2018.11.062.

Huang, Y., Zhu, X., Ding, Z., Lv, G., 2015. [Study on anti-angiogenesis effect of three curcumin pigments and expression of their relevant factors]. Zhongguo Zhongyao Zazhi 40, 324–329.

Huuskes, B.M., DeBuque, R.J., Kerr, P.G., Samuel, C.S., Ricardo, S.D., 2019. The use of live cell imaging and automated image analysis to assist with determining optimal parameters for angiogenic assay in vitro. Front. Cell Dev. Biol. 7, 45. https://doi.org/10.3389/fcell.2019.00045.

Ireson, C., Orr, S., Jones, D.J., Verschoyle, R., Lim, C.K., Luo, J.L., Howells, L., Plummer, S., Jukes, R., Williams, M., Steward, W.P., Gescher, A., 2001. Characterization of metabolites of the chemopreventive agent curcumin in human and rat hepatocytes and in the rat in vivo, and evaluation of their ability to inhibit phorbol ester-induced prostaglandin E2 production. Cancer Res. 61, 1058–1064.

Jiao, D., Wang, J., Lu, W., Tang, X., Chen, J., Mou, H., Chen, Q.-Y., 2016. Curcumin inhibited HGF-induced EMT and angiogenesis through regulating c-Met dependent PI3K/Akt/mTOR signaling pathways in lung cancer. Mol. Ther. Oncolytics 3, 16018. https://doi.org/10.1038/mto.2016.18.

Joshi, P., Joshi, S., Semwal, D., Bisht, A., Paliwal, S., Dwivedi, J., Sharma, S., 2021. Curcumin: an insight into molecular pathways involved in anticancer activity. Mini Rev. Med. Chem. 21, 2420–2457. https://doi.org/10.2174/1389557521666210122153823.

Kalluru, H., Mallayasamy, S.R., Kondaveeti, S.S., Chandrasekhar, V., Kalachaveedu, M., 2022. Effect of turmeric supplementation on the pharmacokinetics of paclitaxel in breast cancer patients: a study with population pharmacokinetics approach. Phytother Res. https://doi.org/10.1002/ptr.7412.

Kao, C.-C., Cheng, Y.-C., Yang, M.-H., Cha, T.-L., Sun, G.-H., Ho, C.-T., Lin, Y.-C., Wang, H.-K., Wu, S.-T., Way, T.-D., 2021. Demethoxycurcumin induces apoptosis in HER2 overexpressing bladder cancer cells through degradation of HER2 and inhibiting the PI3K/Akt pathway. Environ. Toxicol. 36, 2186–2195. https://doi.org/10.1002/tox.23332.

Kettle, J.G., Anjum, R., Barry, E., Bhavsar, D., Brown, C., Boyd, S., Campbell, A., Goldberg, K., Grondine, M., Guichard, S., Hardy, C.J., Hunt, T., Jones, R.D.O., Li, X., Moleva, O., Ogg, D., Overman, R.C., Packer, M.J., Pearson, S., Schimpl, M., Shao, W., Smith, A., Smith, J.M., Stead, D., Stokes, S., Tucker, M., Ye, Y., 2018. Discovery of N-(4-{[5-Fluoro-7-(2-methoxyethoxy)quinazolin-4-yl]amino}phenyl)-2-[4-(propan-2-yl)-1 H-1,2,3-triazol-1-yl]acetamide (AZD3229), a potent pan-KIT mutant inhibitor for the treatment of gastrointestinal stromal tumors. J. Med. Chem. 61, 8797–8810. https://doi.org/10.1021/acs.jmedchem.8b00938.

Kim, J.H., Shim, J.S., Lee, S.-K., Kim, K.-W., Rha, S.Y., Chung, H.C., Kwon, H.J., 2002. Microarray-based analysis of antiangiogenic activity of demethoxycurcumin on human umbilical vein endothelial cells: crucial involvement of the down-regulation of matrix metalloproteinase. Jpn. J. Cancer Res. 93, 1378–1385. https://doi.org/10.1111/j.1349-7006.2002.tb01247.x.

Koo, H.-J., Shin, S., Choi, J.Y., Lee, K.-H., Kim, B.-T., Choe, Y.S., 2015. Introduction of methyl groups at C2 and C6 positions enhances the antiangiogenesis activity of curcumin. Sci. Rep. 5, 14205 https://doi.org/10.1038/srep14205.

Kunihiro, A.G., Brickey, J.A., Frye, J.B., Luis, P.B., Schneider, C., Funk, J.L., 2019. Curcumin, but not curcumin-glucuronide, inhibits Smad signaling in TGFβ-dependent bone metastatic breast cancer cells and is enriched in bone compared to other tissues. J. Nutr. Biochem. 63, 150–156. https://doi.org/10.1016/j.jnutbio.2018.09.021.

Mahale, J., Singh, R., Howells, L.M., Britton, R.G., Khan, S.M., Brown, K., 2018. Detection of plasma curcuminoids from dietary intake of turmeric-containing food in human volunteers. Mol. Nutr. Food Res. 62, e1800267 https://doi.org/10.1002/mnfr.201800267.

Menendez, C., Dueñas, M., Galindo, P., González-Manzano, S., Jimenez, R., Moreno, L., Zarzuelo, M.J., Rodríguez-Gómez, I., Duarte, J., Santos-Buelga, C., Perez-Vizcaino, F., 2011. Vascular deconjugation of quercetin glucuronide: the flavonoid paradox revealed? Mol. Nutr. Food Res. 55, 1780–1790. https://doi.org/10.1002/mnfr.201100378.

Nelson, K.M., Dahlin, J.L., Bisson, J., Graham, J., Pauli, G.F., Walters, M.A., 2017. The essential medicinal chemistry of curcumin. J. Med. Chem. 60, 1620–1637. https://doi.org/10.1021/acs.jmedchem.6b00975.

Núñez-Sánchez, M.A., González-Sarrías, A., Romo-Vaquero, M., García-Villalba, R., Selma, M.V., Tomás-Barberán, F.A., García-Conesa, M.-T., Espín, J.C., 2015. Dietary phenolics against colorectal cancer–From promising preclinical results to poor translation into clinical trials: pitfalls and future needs. Mol. Nutr. Food Res. 59, 1274–1291. https://doi.org/10.1002/mnfr.201400866.

Pan, M.-H., Chiou, Y.-S., Chen, L.-H., Ho, C.-T., 2015. Breast cancer chemoprevention by dietary natural phenolic compounds: specific epigenetic related molecular targets. Mol. Nutr. Food Res. 59, 21–35. https://doi.org/10.1002/mnfr.201400515.

Potente, M., Gerhardt, H., Carmeliet, P., 2011. Basic and therapeutic aspects of angiogenesis. Cell 146, 873–887. https://doi.org/10.1016/j.cell.2011.08.039.

Rajabi, M., Mousa, S.A., 2017. The role of angiogenesis in cancer treatment. Biomedicines 5, E34. https://doi.org/10.3390/biomedicines5020034.

Ramezani, M., Hatamipour, M., Sahebkar, A., 2018. Promising antitumor properties of bisdemethoxycurcumin: a naturally occurring curcumin analogue. J. Cell. Physiol. 233, 880–887. https://doi.org/10.1002/jcp.25795.

Roos, Katarina, Wu, Chuanjie, Damm, Wolfgang, Reboul, Mark, Stevenson, James M., Lu, Chao, Dahlgren, Markus K., Mondal, Sayan, Chen, Wei, Wang, Lingle, Abel, Robert, Friesner, Richard A., Harder, Edward D., 2019. OPLS3e: Extending force field coverage for drug-like small molecules. J. Chem. Theory Comput. 15 (3), 1863–1874. https://doi.org/10.1021/acs.jctc.8b01026.

Seo, H.-R., Jeong, H.E., Joo, H.J., Choi, S.-C., Park, C.-Y., Kim, J.-H., Choi, J.-H., Cui, L.-H., Hong, S.J., Chung, S., Lim, D.-S., 2016. Intrinsic FGF2 and FGF5 promotes angiogenesis of human aortic endothelial cells in 3D microfluidic angiogenesis system. Sci. Rep. 6, 28832 https://doi.org/10.1038/srep28832.

Shakeri, A., Ward, N., Panahi, Y., Sahebkar, A., 2019. Antiangiogenic activity of curcumin in cancer therapy: a narrative review. Curr. Vasc. Pharmacol. 17, 262–269. https://doi.org/10.2174/1570161116666180209113014.

Shankar, S., Chen, Q., Sarva, K., Siddiqui, I., Srivastava, R.K., 2007. Curcumin enhances the apoptosis-inducing potential of TRAIL in prostate cancer cells: molecular mechanisms of apoptosis, migration and angiogenesis. J. Mol. Signal. 2, 10. https://doi.org/10.1186/1750-2187-2-10.

Sharifi-Rad, J., Rayess, Y.E., Rizk, A.A., Sadaka, C., Zgheib, R., Zam, W., Sestito, S., Rapposelli, S., Neffe-Skocińska, K., Zielińska, D., Salehi, B., Setzer, W.N., Dosoky, N. S., Taheri, Y., El Beyrouthy, M., Martorell, M., Ostrander, E.A., Suleria, H.A.R., Cho, W.C., Maroyi, A., Martins, N., 2020. Turmeric and its major compound curcumin on health: bioactive effects and safety profiles for food, pharmaceutical, biotechnological and medicinal applications. Front. Pharmacol. 11, 01021 https://doi.org/10.3389/fphar.2020.01021.

Sheu, M.-J., Lin, H.-Y., Yang, Y.-H., Chou, C.-J., Chien, Y.-C., Wu, T.-S., Wu, C.-H., 2013. Demethoxycurcumin, a major active curcuminoid from Curcuma longa, suppresses balloon injury induced vascular smooth muscle cell migration and neointima formation: an in vitro and in vivo study. Mol. Nutr. Food Res. 57, 1586–1597. https://doi.org/10.1002/mnfr.201200462.

Simon, T., Gagliano, T., Giamas, G., 2017. Direct effects of anti-angiogenic therapies on tumor cells: VEGF signaling. Trends Mol. Med. 23, 282–292. https://doi.org/10.1016/j.molmed.2017.01.002.

Slika, L., Patra, D., 2020. Traditional uses, therapeutic effects and recent advances of curcumin: a mini-review. Mini Rev. Med. Chem. 20, 1072–1082. https://doi.org/10.2174/1389557520666200414161316.

Stroganov, O.V., Novikov, F.N., Stroylov, V.S., Kulkov, V., Chilov, G.G., 2008. Lead finder: an approach to improve accuracy of protein-ligand docking, binding energy estimation, and virtual screening. J. Chem. Inf. Model. 48, 2371–2385. https://doi.org/10.1021/ci800166p.

Tan, P.H., Chan, C., Xue, S.A., Dong, R., Ananthesayanan, B., Manunta, M., Kerouedan, C., Cheshire, N.J.W., Wolfe, J.H., Haskard, D.O., Taylor, K.M., George, A. J.T., 2004. Phenotypic and functional differences between human saphenous vein (HSVEC) and umbilical vein (HUVEC) endothelial cells. Atherosclerosis 173, 171–183. https://doi.org/10.1016/j.atherosclerosis.2003.12.011.

Tapia-Abellán, A., Angosto-Bazarra, D., Martínez-Banaclocha, H., de Torre-Minguela, C., Cerón-Carrasco, J.P., Pérez-Sánchez, H., Arostegui, J.I., Pelegrin, P., 2019. MCC950 closes the active conformation of NLRP3 to an inactive state. Nat. Chem. Biol. 15, 560–564. https://doi.org/10.1038/s41589-019-0278-6.

Trott, O., Olson, A.J., 2010. AutoDock Vina: improving the speed and accuracy of docking with a new scoring function, efficient optimization, and multithreading. J. Comput. Chem. 31, 455–461. https://doi.org/10.1002/jcc.21334.

Wang, D., Chen, Z., Wai Kan Yeung, A., Atanasov, A.G., 2021. Differences between common endothelial cell models (primary human aortic endothelial cells and EA. hy926 cells) revealed through transcriptomics, bioinformatics, and functional analysis. Curr. Res. Biotechnol. 3, 135–145. https://doi.org/10.1016/j.crbiot.2021.05.001.

Wang, T., Chen, J., 2019. Effects of curcumin on vessel formation insight into the pro- and antiangiogenesis of curcumin. Evid. Based Complement Alternat. Med., 1390795 https://doi.org/10.1155/2019/1390795.

Wang, W., Sukamtoh, E., Xiao, H., Zhang, G., 2015. Curcumin inhibits lymphangiogenesis in vitro and in vivo. Mol. Nutr. Food Res. 59, 2345–2354. https://doi.org/10.1002/mnfr.201500399.

Wang, X., Bove, A.M., Simone, G., Ma, B., 2020. Molecular bases of VEGFR-2-mediated physiological function and pathological role. Front. Cell Dev. Biol. 8, 599281 https://doi.org/10.3389/fcell.2020.599281.

Yadav, V.R., Aggarwal, B.B., 2011. Curcumin: a component of the golden spice, targets multiple angiogenic pathways. Cancer Biol. Ther. 11, 236–241. https://doi.org/10.4161/cbt.11.2.14405.

Yoon, M.J., Kang, Y.J., Lee, J.A., Kim, I.Y., Kim, M.A., Lee, Y.S., Park, J.H., Lee, B.Y., Kim, I.A., Kim, H.S., Kim, S.-A., Yoon, A.-R., Yun, C.-O., Kim, E.-Y., Lee, K., Choi, K. S., 2014. Stronger proteasomal inhibition and higher CHOP induction are responsible for more effective induction of paraptosis by dimethoxycurcumin than curcumin. Cell Death Dis. 5, e1112. https://doi.org/10.1038/cddis.2014.85.

Yoysungnoen, P., Wirachwong, P., Bhattarakosol, P., Niimi, H., Patumraj, S., 2006. Effects of curcumin on tumor angiogenesis and biomarkers, COX-2 and VEGF, in hepatocellular carcinoma cell-implanted nude mice. Clin. Hemorheol. Microcirc. 34, 109–115.

Yoysungnoen-Chintana, P., Bhattarakosol, P., Patumraj, S., 2014. Antitumor and antiangiogenic activities of curcumin in cervical cancer xenografts in nude mice. BioMed Res. Int., 817972 https://doi.org/10.1155/2014/817972.